Am J Physiol Lung Cell Mol Physiol 295: L789–L799, 2008.
First published September 5, 2008; doi:10.1152/ajplung.90306.2008.

High levels of hyaluronan in idiopathic pulmonary arterial hypertension

Metin Aytekin,[1] Suzy A. A. Comhair,[1] Carol de la Motte,[1] Sudip K. Bandyopadhyay,[1] Carol F. Farver,[3] Vincent C. Hascall,[2] Serpil C. Erzurum,[1,4] and Raed A. Dweik[1,4]

Departments of [1]Pathobiology and [2]Biomedical Engineering, Lerner Research Institute, and Departments of [3]Pathology and [4]Pulmonary and Critical Care Medicine, Respiratory Institute, Cleveland Clinic, Cleveland, Ohio

Submitted 9 May 2008; accepted in final form 29 August 2008

Aytekin M, Comhair SA, de la Motte C, Bandyopadhyay SK, Farver CF, Hascall VC, Erzurum SC, Dweik RA. High levels of hyaluronan in idiopathic pulmonary arterial hypertension. *Am J Physiol Lung Cell Mol Physiol* 295: L789–L799, 2008. First published September 5, 2008; doi:10.1152/ajplung.90306.2008.—Hyaluronan (HA), a large glycosaminoglycan found in the ECM, has major roles in lung and vascular biology and disease. However, its role in idiopathic pulmonary arterial hypertension (IPAH) is unknown. We hypothesized that HA metabolism is abnormal in IPAH. We measured the plasma levels of HA in IPAH and healthy individuals. We also evaluated HA synthesis and the expression of HA synthases and hyaluronidases in pulmonary artery smooth muscle cells (PASMCs) from explanted lungs. Plasma HA levels were markedly elevated in IPAH compared with controls [HA (ng/ml, mean ± SD): IPAH 325 ± 80, control 28 ± 9; $P = 0.02$]. In vitro, unstimulated IPAH PASMCs produced high levels of HA compared with control cells [HA in supernatant (μg/ml, mean ± SD): IPAH 12 ± 2, controls 6 ± 0.9; $P = 0.04$]. HA levels were also higher in IPAH PASMC lysates. The increased HA was biologically relevant as shown by tissue staining and increased HA-specific binding of mononuclear cells to IPAH compared with control PASMCs [number of bound cells × 10^4 (mean ± SD): IPAH 9.5 ± 3, control 3.0 ± 1; $P = 0.01$]. This binding was abrogated by the addition of hyaluronidase. HA synthase-2 and hyaluronidase-2 were predominant in control and IPAH PASMCs. Interestingly, the expressions of HA synthase-2 and hyaluronidase-2 were ~2-fold lower in IPAH compared with controls [HA synthase-2 (relative expression mean ± SE): IPAH 4.3 ± 0.02, control 7.8 ± 0.1; $P = 0.0004$; hyaluronidase-2 (relative expression mean ± SE): IPAH 4.2 ± 0.06, control 7.6 ± 0.07; $P = 0.008$]. Thus patients with IPAH have higher circulating levels of HA, and PASMCs derived from IPAH lungs produce more HA compared with controls. This is associated with increased tissue levels and increased binding of inflammatory cells suggesting a role for HA in remodeling and inflammation in IPAH.

hyaluronidase; lung; remodeling

IDIOPATHIC PULMONARY ARTERIAL hypertension (IPAH) is a progressive disease that leads to deterioration in cardiopulmonary function and premature death from right ventricular failure (14, 17, 24, 26). Whereas the pathogenesis of IPAH is not entirely known, the main processes believed to lead to progressive pulmonary arterial narrowing include vasoconstriction, in situ thrombosis, cellular proliferation, and ultimately vascular remodeling (14, 17, 24, 26). Although pulmonary artery smooth muscle cells (PASMCs) are considered a major component of the remodeling process in IPAH, the nature of the primary abnormality that triggers and perpetuates PASMC proliferation in IPAH is unclear. ECM has important roles in cell proliferation and migration. The integrity and balance of matrix components are essential for normal lung function and response to injury. Identifying matrix abnormalities in IPAH will help us better understand the disease pathobiology and may help efforts to resolve or reverse the disease process. Different lung diseases, like asthma, emphysema, and pulmonary fibrosis, are associated with abnormal ECM turnover (45). There are several different components in the ECM of the lung, including proteoglycans, elastin, and collagen. Proteoglycans consist of a core protein to which one or more glycosaminoglycan chains (GAGs) are attached. GAGs present in the lung include hyaluronan (HA), heparan sulfate, dermatan sulfate, and chondroitin sulfate (39). In addition to their importance for organ structure, matrix components are involved in mediating a variety of physiological and pathological processes. HA degradation products can induce the expression of a variety of genes, chemokines, cytokines, growth factors, signal transduction molecules, and adhesion molecules (43). Furthermore, HA degradation products can stimulate angiogenesis (50).

HA is a large glycosaminoglycan composed of repeats of two alternating sugar units, β-D-*N*-acetylglucosamine and β-D-glucuronate, and is part of pericellular and extracellular matrices. It is present in synovial fluids, the vitreous body, and several other tissues including the lungs (3). HA is synthesized by HA synthases (HAS), a group of three cell transmembrane proteins: HAS1, HAS2, and HAS3. These enzymes lengthen HA by repeatedly adding glucuronic acid and *N*-acetylglucosamine alternately to the nascent chain as it is extruded through the cell membrane into the extracellular space (25, 38). HAS expression is context specific according to cell type. All inhibitors of protein synthesis such as cycloheximide treatment, endoplasmic reticulum (ER) stress, and double-stranded RNA induce HA production in smooth muscle cells (SMCs) (20). The synthesis of HA is also increased in SMCs after viral infection or treatment with polyinosinic acid:polycytidylic acid [poly(I:C)], a synthetic double-stranded RNA that initiates responses similar to viral infection (9, 20).

Whereas it is abundant in extracellular matrices, HA also contributes to proliferation of cells and participates in a number of cell surface receptor interactions, including its primary receptor, CD44. The contribution of HA to cell proliferation may be due to its interaction with CD44, which participates in cell adhesion interactions required by proliferating cells. The binding of CD44 to HA stimulates angiogenesis and aggregation, proliferation, and migration of cells (6, 10, 13, 28). There is also evidence that HA degradation products may have inflammatory properties independent of interaction with CD44 (43).

Address for reprint requests and other correspondence: R. A. Dweik, Dept. of Pulmonary and Critical Care Medicine, Respiratory Institute, Desk A-90, Cleveland Clinic, 9500 Euclid Ave., Cleveland, OH 44195 (e-mail: dweikr@ccf.org).

The costs of publication of this article were defrayed in part by the payment of page charges. The article must therefore be hereby marked "*advertisement*" in accordance with 18 U.S.C. Section 1734 solely to indicate this fact.

Thus HA has important roles in the lung response to injury and other pathobiological processes implicated in IPAH, including angiogenesis, vascular remodeling, and cell proliferation and migration. However, the role of HA in IPAH has not been studied previously. Here, we present the novel finding that IPAH patients have high levels of circulating HA. Our data also show that one possible source of HA is PASMCs from IPAH lungs, which, unlike PASMCs from controls, spontaneously produce high levels of HA without stimulation and make HA cables that have the functional ability to bind inflammatory cells. Our data suggest a potential role for HA in remodeling and the interaction between inflammatory cells and SMCs in IPAH that contributes to the pathobiology of the disease.

EXPERIMENTAL PROCEDURES

Study population. The study included 22 patients with IPAH identified based on the National Institutes of Health (NIH) registry diagnostic criteria for pulmonary hypertension subclass 1.1 according to the World Health Organization criteria (17, 40) and 9 healthy control volunteers. Demographic and clinical characteristics of the IPAH individuals are listed in Table 1. The healthy controls (mean age 32 ± 2 yr, 6 female) were individuals with no history of pulmonary or cardiac disease or symptoms. The study was approved by the Cleveland Clinic Institutional Review Board (IRB), and all participants signed an IRB-approved consent form before participation in the study.

HA. Levels of HA in plasma or conditioned media were measured with a commercial competitive binding kit (cat. no. DY3614; R&D Systems, Minneapolis, MN). In these experimental conditions, the lowest detectable level of HA was 1.15 ng/ml. The assay was used according to manufacturer's instructions.

Cell preparation and isolation. Human PASMC were isolated from elastic pulmonary arteries (>500-μm diameter) dissected from lungs obtained at explantation during lung transplant. After removal of endothelial cells, PASMCs were dissociated by digestion with collagenase type II/DNase I solution overnight at 37°C (52). Cells were cultured on uncoated plates in SMC growth medium (SmGM-2; Cambrex) containing 5% glucose, 10% FBS, and 5% Antibiotic-Antimycotic from GIBCO (cat. no. 15240). Cells were passaged at 60–90% confluence by dissociation from plates with 0.05% trypsin and 0.53 mM EDTA. Primary cultures of *passages 5-8* were used in experiments. The smooth muscle phenotype of cultured cells was confirmed (>97% purity) by immunohistochemistry and flow cytometric analysis with antibodies against smooth muscle α-actin and calponin.

Table 1. *Demographics and clinical characteristics of IPAH study subjects*

	Subjects With IPAH
n	22
Mean age, yr	46 ± 3.3
Sex (F/M)	21/1
FEV_1, l	2.4 ± 0.2
FEV_1 (% of predicted)	82.9 ± 4.4
FVC, l	3.1 ± 0.2
FVC (% of predicted)	91.5 ± 3.8
MPAP, mmHg	94.7 ± 2.7
PVR, Wood units	12.7 ± 1.7
CI, l/min/m^2	2.2 ± 0.2
AST, mg/dl	281 ± 144
ALT, mg/dl	121 ± 58
Bilirubin, mg/dl	0.7 ± 0.1
Creatinine, mg/dl	1.0 ± 0.1
Medications	No. of patients
Oxygen	8
Coumadin	11
Diuretic	10
Digoxin	11
Calcium channel blocker	5
Prostanoid	11
Endothelin blocker	10
Phosphodiesterase inhibitor	3

Values are means ± SE. IPAH, idiopathic pulmonary arterial hypertension; F/M, female/male; FEV_1, forced expiratory volume in 1 s; FVC, forced vital capacity; MPAP, mean pulmonary arterial pressure; PVR, pulmonary vascular resistance; CI, cardiac index; AST, aspartate aminotransferase; ALT, alanine aminotransferase.

Histological studies. Lung tissues were taken from explanted lungs and fixed and embedded in paraffin, and 4-μm sections were prepared. The sections were stained with hematoxylin and eosin (H&E) for morphological examination.

Immunostaining. In cell culture, staining was done to detect HA by a HA binding protein probe (cat. no. 385911; Calbiochem). PASMCs were seeded on culture slides (BD Falcon, Bedford, MA). Slides were rinsed once with HBSS, fixed in −20°C methanol, and air dried. The culture slides were preincubated with HBSS with 2% FBS for 30 min at room temperature. After discarding the medium, culture slides were incubated in HBSS with biotinylated HA binding protein at the recommended dilutions overnight at 4°C on a wet towel to prevent drying. After overnight incubation, the culture slides were washed three times with HBSS without FBS and then incubated with fluorescein-tagged streptavidin (1:500) in HBSS with 2% FBS for 60 min at room temperature. The culture slides were washed three times with HBSS without FBS and mounted with Vectashield mounting medium containing 4,6-diamidino-2-phenylindole (DAPI; Vector Laboratories, Burlingame, CA). The edges of culture slides were then sealed with nail polish, and the slides kept were at −20°C. Fluorescence images were collected using an HCX PL APO ×40/numerical aperture (NA) 1.25 oil-immersion objective on a Leica DMR upright microscope (Leica Microsystems, Wetzlar, Germany) equipped with a Retiga EXi Cooled CCD Camera (QImaging, Burnaby, British Columbia, Canada) and Image Pro Plus software (Media Cybernetics, Silver Spring, MD).

In lung tissue, HA was also detected by the same HA binding protein probe used as described above. SMCs were stained with monoclonal anti-smooth muscle actin antibody (cat. no. A 2547; Sigma-Aldrich), and endothelial cells were stained with polyclonal rabbit anti-human von Willebrand factor (vWF) antibody (cat. no. A0082; Dako). Confocal images were collected using an HC PL APO ×20/0.7 NA or HCX PL APO ×40/1.25 NA objective lens on a Leica TCS SP2 AOBS spectral confocal microscope (Leica-Microsystems). The excitation (Ex)/emission (Em) wavelengths were as follows: DAPI, Ex 351 nm, Em 400–480 nm; Alexa Fluor 488, Ex 488 nm, Em 500–550 nm; Alexa Fluor 568, Ex 561 nm, Em 570–630 nm; Alexa Fluor 633, Ex 633 nm, Em 640–800.

Fluorophore-assisted carbohydrate electrophoresis assays. Proteinase K digestion of cell layer fractions: PASMCs were grown in 6-well plates until they reached ~90% confluence. Some cultures were treated with poly(I:C) (20 μg/ml) for 18 h before the assay. The cells in 6-well plates were kept at −20°C until digestion with proteinase K (cat. no. 25530-015; Invitrogen, Carlsbad, CA). For proteinase K digestion, 100 mM ammonium acetate, pH 7, was added to each well. Proteinase K (125 μg/ml) was added and incubated at 60°C for 2 h with mixing every 30 min. Afterward, another 125 μg/ml proteinase K was added followed by incubation for another 2 h. The digests were transferred to 1.5 ml microcentrifuge tubes and concentrated by vacuum centrifugation to ~250 μl. One milliliter of −20°C 100% alcohol was added to each sample followed by vortexing and overnight incubation at −20°C. Samples were then centrifuged at 14,000 *g* for 20 min. After discarding the supernatant, pellets were washed with 1 ml, −20°C, 75% alcohol. Samples were centrifuged again at 14,000 *g* for 20 min, and the pellets were air dried at room

temperature after discarding the supernatants. Ammonium acetate (0.1 M, pH 7) was added to each sample followed by incubation at room temperature for 20 min. Samples were placed in a boiling water bath for 5 min to destroy remaining proteinase K.

Chondroitinase and hyaluronidase digestion. An amount of 0.6 μl of 1% glacial acetic acid was added to each sample to optimize enzymatic action at pH 5–6. Hyaluronidase and chondroitinase ABC (cat. nos. 100741-1A and 100330-1A, respectively; Seikagaku) were pooled together in a 1:1 ratio, and 3.2 μl of the enzyme mixture was added to each sample followed by incubation at 37°C for 3 h. The enzymes were heat inactivated as described for proteinase K. Alcohol (160 μl, −20°C, 100%) was added to each sample, and the samples were incubated overnight at −80°C. They were then centrifuged at 14,000 *g* for 20 min. Supernatants that contained disaccharide digestion products from HA and chondroitin sulfate were dried by centrifugal evaporation in microtubes. A solution containing 12.5 mM 2-aminoacridone (AMAC; cat. no. A-6289; Molecular Probes), 7.5% glacial acetic acid, and 0.5 M cyanoborohydride (cat. no. 15.615-9; Sigma-Aldrich) was added to each sample followed by incubation overnight at 37°C in the dark.

Fluorophore-assisted carbohydrate electrophoresis analysis. At the end of the incubation, the samples were each mixed with 80% glycerol (cat. no. BP 229-1; Fisher Chemicals). Each sample was subjected to electrophoresis on mono composition gels with mono running buffer (300 V at 4°C for 1 h). An ultra Lum transilluminator (365 nm) was used for gel imaging, and a Quantix cooled charge-coupled device camera (Roper Scientific/Photometrics) was used to capture images by the Gel-Pro Analyzer program version 3.0 (Media Cybernetics). ImageJ (version 1.38x; NIH) was used to analyze the images.

Assay for monocyte adhesion. Monocyte binding to PASMCs was quantified as previously described (8, 9). PASMCs were grown to confluence in 24-well plates. Treatment with poly(I:C) as a positive control (20 μg/ml) was done 18 h before assay. Up to 70×10^6 U937 cells per milliliter were labeled for 90 min at 37°C with 100 μCi ^{51}Cr as sodium chromate (PerkinElmer Life Sciences) in 1 ml of RPMI with 10% FBS. The radiolabeled U937 cells were washed three times with culture medium without serum. After washing, the cells were resuspended to 1×10^6/0.5 ml. U937 (1×10^6 labeled) cells were added to each well followed by incubation for 1 h at 4°C for the binding phase. All cultures were washed once with cold, serum-free medium. To determine whether the binding is mediated through HA, 200 μg/ml hyaluronidase (cat. no. H4272; Sigma-Aldrich) was added in certain wells. All wells were washed two more times with cold medium to remove nonadherent monocytes before lysis by 200 μl of 1% Triton X-100. One hundred microliters of 1% Triton X-100 was removed for quantification of radioactivity by 1470 Automatic Gamma Counter from PerkinElmer. The number of U937 cells per well was calculated from the initial specific activity (8).

cDNA synthesis and real-time quantitative PCR. Real-time quantitative PCR (RTQ-RT-PCR) was used to quantitatively measure hyaluronidase-1 (HYAL1), HYAL2, HAS1, HAS2, and HAS3 mRNA expression in normal and IPAH PASMCs. RNA was isolated from PASMCs obtained from explanted lungs. For cDNA synthesis, 1 μg of each RNA sample was digested with DNase I (Roche Diagnostics, Mannheim, Germany), and the respective mRNA probes were synthesized using an oligo(dT) primer and MLV (cat. no. 18418-020; Invitrogen). SYBR Green Technology (cat. no. 4309155; Applied Biosystems, Warrington, United Kingdom) was done for all RTQ-RT-PCR experiments. Reactions were done in an iCycler Thermal Cycler (Bio-Rad) in a total volume of 20 μl using the annealing temperature in Table 2. Expressions of HYALs and HASs mRNA relative to the housekeeping gene GAPDH were calculated using the $\Delta\Delta C_t$ method (31). The PCR conditions were 1 cycle at 50°C for 2 min, 1 cycle at 95°C for 10 min, followed by 40 cycles of 95°C for 15 s and 65°C for 1 min for all primers. HYAL1 and HYAL2 primers were described previously (37).

Western blot. Expression of KDEL (Lys-Asp-Glu-Leu) and hyaluronidase in PASMCs was evaluated by Western blot analysis. PASMCs from the patients with IPAH and control were cultured on p100 cell culture plates until they reached 70% confluence. The cells were removed from the plates, pelleted by centrifugation, and lysed for 30 min on ice in a lysis buffer (50 mM Tris, pH 7.4, 100 mM NaCl, 1 mM EDTA, 1% Nonidet P-40, and 10% glycerol) containing 10 μg/ml pepstatin, 1 mM PMSF, 1 mM DTT, 20 μg/ml aprotinin, 5 μg/ml leupeptin, and 1 μM sodium orthovanadate. The cell lysates were incubated at 95°C for 10 min with a 1% SDS-PAGE sample buffer with 10% 2-mercaptoethanol. SDS-PAGE was done using 4–15% gradient gels. The proteins were transferred to nitrocellulose as described previously (53), incubated with the primary anti-KDEL antibody or hyaluronidase antibody, and developed using enhanced chemiluminescence (ECL) (Amersham). The antibodies used were the mouse anti-KDEL antibody (dilution 1:1,000) purchased from Stressgen Biotechnologies (Victoria, Canada) and the rabbit anti-HYAL2 antibody (dilution 1:500; a generous gift from Robert Stern, University of California, San Francisco).

HA sizing. PASMCs were lysed with 2% CHAPS (in 0.05 M Tris, pH 7.0) for 5 min. An equal volume of 8 M guanidine HCl (in 0.05 M Tris, pH 7.0, and 1% CHAPS) was added. Cell lysates were incubated overnight at −20°C after adding 4× cold 200 proof ethanol. Samples were centrifuged at 14,000 *g* for 10 min and washed with 75% ethanol. After air drying for 20 min they were resuspended in 100 mM ammonium acetate (pH 7.0) for 20 min at room temperature. To remove all traces of guanidine HCl, the ethanol precipitation step

Table 2. *List of primers used in RTQ-RT-PCR*

Primers	Sequence	GenBank Acc. No.	Nucleotide Position, bp
hHAS1 fwd	CCT GCA TCA GCG GTC CTC TA	NM_001523	943–962
hHAS1 rev	GCC GGT CA-T CCC CAA AAG 3	NM_001523	1056–1039
hHAS2 fwd	CGC AAC ACG TAA CGC AAT TGG	NM_005328	1038–1058
hHAS2 rev	CCA CAG ATG AGG CTG GGT CAA G	NM_005328	1184–1205
hHAS3 fwd	GGC GAT TCG GTG GAC TAC ATC C	AF232772	769–790
hHAS3 rev	ACG CTG CTC AGG AAG GAA ATC C	AF232772	917–938
hHyal-1 fwd	GTA TGT GCA ACA CCG TGT GGC	HSU96078	1390–1410
hHyal-1 rev	CAG GCG TGA GCT GGA TGG AGA	HSU96078	1790–1770
hHyal-2 fwd	CCA TGC ACT CCC AGT CTA CGT C	BC000692	1004–1025
hHyal-2 rev	TCA CCC CAG AGG ATG ACA CCA G	BC000692	1138–1117
hGAPDH fwd	ACC ACA GTC CAT GCC ATC AC	X54989	167–144
hGAPDH rev	TCC ACC ACC CTG TTG CTG TA	X54989	2456–2481

Shown are the names, sequences, source sequence accession numbers, and relative positions of the primers used for real-time quantitative PCR (RTQ-RT-PCR). The annealing temperature for all RTQ-RT-PCR primers was 65°C. The letter h in front of primer names designates primers specific for human genes. HAS, hyaluronan synthase; Hyal, hyaluronidase; fwd, forward primer; rev, reverse primer.

was repeated. After the second ethanol precipitation, the pellet was digested with 1 mg/ml protease K in 0.01% SDS at 60°C overnight followed by SpeedVac to 250 μl and adding 1 ml of cold absolute ethanol and incubating at −20°C overnight. After repeating ethanol precipitation, 100 μl of 100 mM ammonium acetate (pH 7.0) was added, and protease activity was destroyed by heating the samples at 100°C for 5 min. One of each sample was used to quantify DNA with the PicoGreen dsDNA quantification reagent (cat. no. P-11496; Molecular Probes). Samples were digested with 0.06 U/μl DNase (cat. no. 2224; Ambion) and 0.04 μg/μl RNase A (cat. no. 109169; Roche Diagnostics) overnight at 37°C. After repeating the precipitation step, samples were resuspended in 20 μl of 100 mM ammonium acetate (pH 7.0). Samples were then divided in half, and 1 μl of hyaluronidase (cat. no. 100740-1; Seikagaku) was added to one-half of each sample and incubated overnight at 37°C for a negative control. The samples were dried by SpeedVac and resuspended in 10 μl of 1× TAE buffer. Samples were subjected to electrophoresis on a 1% agarose gel alongside HA standards of different sizes, mega molecular mass HA (6,100, 4,570, 3,050, and 1,520 kDa), high molecular mass HA (1,510, 1,090, 966, 572, and 495 kDa), and lower molecular mass HA (495, 310, 214, and 110 kDa). The gel was stained with 0.005% Stain-All overnight and then destained with water until clear before a picture was taken.

Hyaluronidase activity. Hyaluronidase activity was detected by HA zymography. Plasma from IPAH and control patients were diluted with 10 volumes of 0.15 M NaCl. The diluted samples were mixed with an equal volume of Laemmli sample buffer containing 4% SDS and no reducing reagent. The mixtures were applied to 8% SDS-polyacrylamide gels containing 0.17 mg/ml HA. After electrophoresis at 25 mA, the gels were rinsed with 2.5% Triton X-100 for 2 h at room temperature. The gels were incubated with fresh incubation buffer (0.1 M sodium formate and 0.15 M NaCl at pH 3.5) 16 h at 37°C. Following incubation, the gels were rinsed with water and incubated with 0.1 μg/ml Actinase E in 20 mM Tris·HCl (pH 8.0) for 2 h at 37°C. The gels were rinsed again and incubated with 0.5% Alcian blue in 25% ethanol and 10% acetic acid for 30 min and destained with 25% ethanol and 10% acetic acid. Gels were photographed, and the agarose gel images were analyzed with ImageJ (NIH, Bethesda, MD).

Statistical analysis. All statistical analysis was done using JMP version 5.0.1.2 for Microsoft Windows. Continuous variables were compared with the independent two-tailed *t*-test. $P \leq 0.05$ was considered as significant.

RESULTS

HA levels in plasma of patients with IPAH and healthy control individuals. HA concentrations in plasma were measured in 22 IPAH and 9 control individuals. As shown in Fig. 1*A*, plasma levels of HA in IPAH patients were markedly higher compared with controls [HA (ng/ml, mean ± SD): IPAH 325 ± 80, controls 28 ± 9; $P = 0.02$].

HA in IPAH and control lung tissues. To evaluate the presence and location of HA in IPAH lung tissue, we stained tissues from three explanted IPAH lungs and three control lungs. Figure 2 shows histopathology and immunostaining of similar size (100–200 μm) arteries from IPAH and control lungs. In addition to H&E staining (Fig. 2, *A* and *B*), the same tissue sections were also stained for cell nuclei (DAPI), SMCs (smooth muscle actin), endothelial cells (vWF), and HA (HA binding protein) (Fig. 2, *G* and *H*). Although this method of HA staining is not quantitative, there appeared to be more intense HA staining (green) around the pulmonary arteries in IPAH (Fig. 2, *C* and *G*) compared with controls (Fig. 2, *D* and *H*). The negative controls, stained with the secondary antibody only, showed slight background auto-fluorescence in the elastic lamina, which is expected (Fig. 2, *E* and *F*). Figure 3 shows the same staining of a plexogenic lesion in an IPAH lung. Although there is widespread staining for HA (green) surrounding the lesion, the area of most intense staining seems to correlate to areas of new collagen deposition on the H&E staining (closed arrows in Fig. 3, *A–C*).

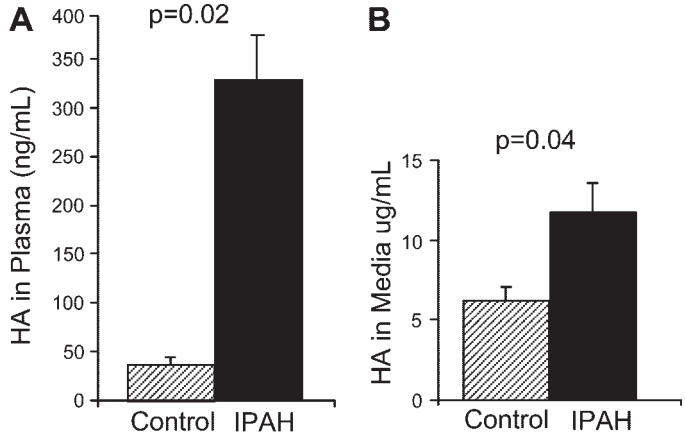

Fig. 1. High levels of hyaluronan (HA) in idiopathic pulmonary arterial hypertension (IPAH). Plasma HA levels were measured by competitive binding assay in 9 healthy individuals and in 22 IPAH patients. HA levels were also measured in conditioned media of pulmonary artery smooth muscle cells (PASMCs) from IPAH and control lungs. Plasma HA in IPAH patients was significantly higher compared with healthy controls (*A*). IPAH PASMC supernatants contained higher levels of HA than control cells (*B*).

Unstimulated IPAH PASMCs produce high levels of HA compared with controls. HA concentrations in the supernatants of three IPAH and three healthy control PASMC cultures were determined by the same method used for plasma. HA levels in the supernatants of PASMCs were significantly higher in IPAH cells compared with healthy controls: [HA (μg/ml, mean ± SD): IPAH 12 ± 2, controls 6 ± 0.9; $P = 0.04$; Fig. 1*B*]. Fluorescence light microscopic imaging was also used to qualitatively determine the synthesis of HA cables in IPAH and control PASMCs. Immunofluorescence pictures (Fig. 4, *A* and *B*) of fixed PASMCs from IPAH and control samples show that IPAH PASMCs produce more HA. Unstimulated IPAH PASMCs produced HA in the pericellular coat (Fig. 4, *A* and *B*, arrowheads) and in extracellular cables (Fig. 4, *A* and *B*, arrows). To quantify the difference in HA production between IPAH and control PASMCs, HA levels were measured by fluorophore-assisted carbohydrate electrophoreses (FACE). Without any treatment each cell layer was harvested, and the glycosaminoglycans were digested to disaccharides. After labeling the disaccharides fluorescently, they were subjected to electrophoresis. Figure 4*C* demonstrates that IPAH PASMCs have significantly higher HA levels compared with control PASMCs. Image density on FACE gel (mean ± SD): IPAH 10,800 ± 2,000, controls 5,200 ± 880; $P = 0.001$ (Fig. 4*D*).

Inflammatory cells bind to HA produced by IPAH PASMCs. As shown in Fig. 5, *A* and *B*, U937 cells from a monocytic cell line (Fig. 5, *A* and *B*, open arrows) bind to HA cables (Fig. 5, *A* and *B*, closed arrows) produced consistently by IPAH PASMCs. There are few cables produced by PASMCs from control lungs and hence limited or no U937 cell binding. We confirmed this qualitative observation by quantifying the bind-

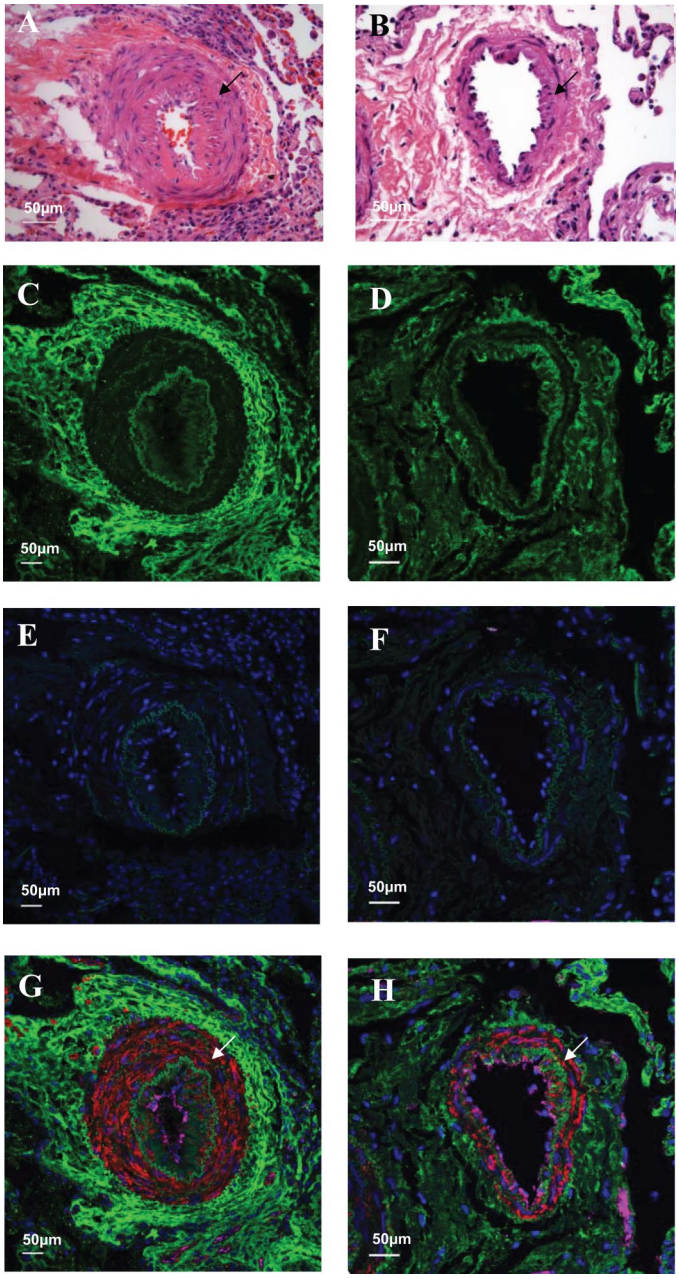

Fig. 2. Lung tissues from IPAH (*left*) and control (*right*) lungs were stained for HA (HA binding protein), smooth muscle cells (SMCs; smooth muscle actin), and endothelial cells (von Willebrand factor) subjects. The pictures focus on small (100–200 μm) pulmonary arterioles. Hematoxylin and eosin (H&E) staining demonstrates the expected smooth muscle hypertrophy and hyperplasia in the IPAH arteriole (arrow in *A*) compared with control (arrow in *B*). There is more intense HA (green) staining surrounding the IPAH arteriole (*C*) compared with the control (*D*). *E* and *F* are negative controls of the same sections stained by the secondary antibody only. The minimal green staining here represents autofluorescence by the elastica, and the blue staining represents the 4,6-diamidino-2-phenylindole (DAPI) staining of the nuclei. *G* and *H* are composite pictures of SMC (red), HA (green), and endothelial cells (purple) for the same sections of IPAH and control lung tissues, respectively.

ing of radiolabeled leukocytes in an adhesion assay (43) as shown in Fig. 5*C*. U937 binding to IPAH PASMCs was more than threefold higher compared with control PASMCs [number of bound cells $\times 10^4$ (mean ± SD): IPAH 9.5 ± 3, control 3.0 ± 1; $P = 0.01$]. Mononuclear cell binding was increased by poly(I:C) treatment of IPAH and control to the same level. This binding is HA specific as it is abrogated by bovine testicular hyaluronidase treatment (Fig. 5*C*).

Expression of HASs in PASMCs. Because the results of conventional PCR did not yield robust signals (data not shown), we used RTQ-RT-PCR to assess the expression HAS levels in PASMCs from three different control and three different IPAH lungs. The primer sequences used to detect HAS1, HAS2, and HAS3 and their accession numbers are shown in Table 2. HAS2 was the predominantly expressed enzyme in both IPAH and control PASMCs with levels that are ~10 times higher than either HAS1 or HAS3. Interestingly, HAS2 expression in IPAH PASMCs was only about half of the levels seen in control PASMCs [HAS2: IPAH 4.3 ± 0.02, control 7.8 ± 0.1; $P = 0.0004$; Fig. 6*A*]. Thus high HA contents in IPAH PASMCs are not explained by differences in HAS mRNA expression.

Expression of hyaluronidase isoforms in PASMCs. We examined hyaluronidase isoforms (HYAL1 and HYAL2) expression in PASMCs cultures derived from three control and three IPAH lungs by RTQ-RT-PCR. The primer sequences used to detect HYAL1 and HYAL2 isoforms and their accession numbers are shown in Table 2. HYAL2 expression was significantly higher than HYAL1 expression in both IPAH and control PASMCs ($P < 0.001$). Interestingly, the expression

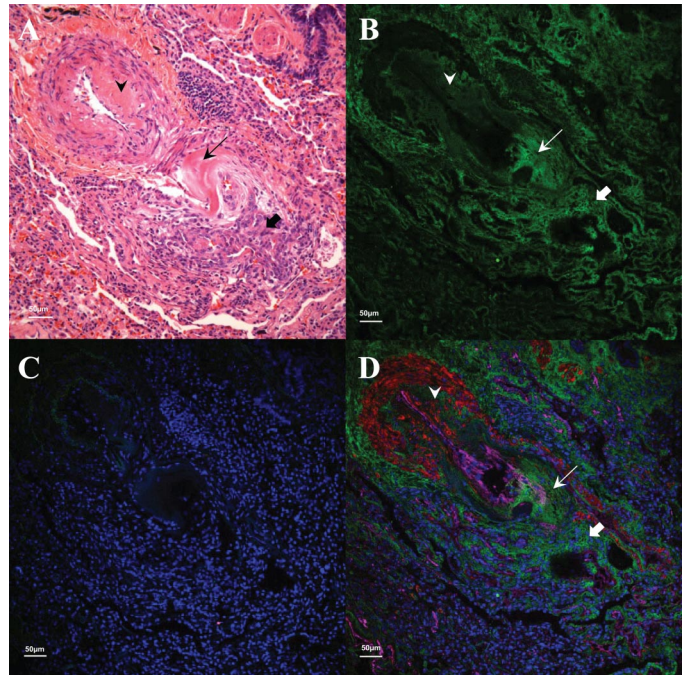

Fig. 3. HA in a plexogenic IPAH lesion. Tissues were stained similar to Fig. 3: lungs were stained for HA (HA binding protein), SMCs (smooth muscle actin), and endothelial cells (von Willebrand factor). H&E staining in *A* demonstrates the typical features of a plexogenic lesion including focal medial sclerosis (arrowhead) with adjacent ectatic arterial segments that lead into the slit-like vascular spaces (thick arrow). There is also an area of medial destruction with new collagen deposition (arrow). *B* shows the HA staining HA, and *C* is the negative control section stained with the secondary antibody only. *D* is a composite picture of SMC (red), HA (green), and endothelia cells (purple) of the same sections. Although there is widespread staining for HA (green) surrounding the lesion, the area of most intense staining seems to correlate to areas of medial destruction with new collagen deposition on the H&E staining (closed arrows in *A*–*C*).

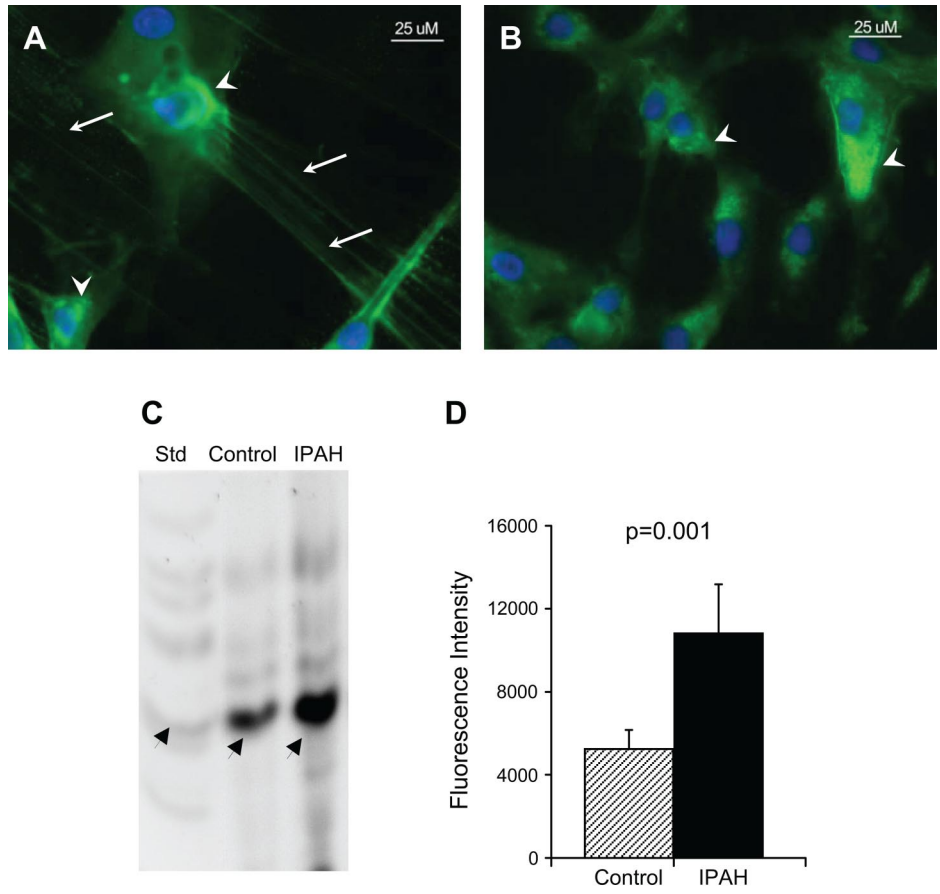

Fig. 4. Increased HA production by unstimulated IPAH PASMCs. Fluorescence light microscopic images of HA in monolayers of PASMCs from IPAH (*A*) and healthy control (*B*) lungs. Nuclei are blue (DAPI stain), and HA is green revealing the pericellular coats (arrowheads in IPAH and control cells) and extracellular cable structures (arrows in IPAH cells). IPAH cells produce distinct HA cables that are not seen in control cells. HA levels were quantified in cell lysates by fluorophore-assisted carbohydrate electrophoreses (FACE). Standard ladder (Std) shows the different sugar components, and arrows mark HA (*C*). The *P* value for the fluorescence intensities and standard errors were calculated from 4 experiments each done in triplicate (*D*).

level of HYAL2 in IPAH PASMCs was significantly lower compared with levels in control PASMCs [HYAL2: IPAH 4.2 ± 0.06, control 7.6 ± 0.07; $P = 0.008$; Fig. 6*B*]. This suggests that decreased degradation of HA may contribute to the high levels of HA in IPAH.

Protein levels of hyaluronidase. We examined hyaluronidase protein levels in PASMC cultures derived from three control and three IPAH lungs by Western blot analyses. The protein levels of hyaluronidase in IPAH PASMCs were similar to control PASMCs (Fig. 7).

Hyaluronidase activity. In vivo plasma hyaluronidase activity was significantly lower in IPAH individuals compared with controls [image density on hyaluronidase activity gel (mean ± SD): controls 71,955 ± 4,104, IPAH 53,998 ± 7,125; $P = 0.04$; Fig. 8, *A* and *B*]. In vitro hyaluronidase activity was also lower in the supernatants from IPAH compared with control PASMCs [image density on hyaluronidase activity gel (mean ± SD): controls 33,889 ± 2,141, IPAH 26,938 ± 937; $P = 0.04$; Fig. 8, *C* and *D*]. These suggest that high level of HA in IPAH patients could be due to low activity of hyaluronidase.

HA sizing. Since the size of HA can determine its physiological effects, we evaluated the size of HA produced by PASMCs. The size of HA was similar (range 3,050–4,570 kDa) in the cell lysates of IPAH and control PASMCs (Fig. 9). In IPAH, there was also another less intense band in the range of 110–214 kDa. The HA levels were higher in IPAH despite equal loading of samples (DNA: IPAH PASMCs 0.261 μg/ml, control PASMCs 0.219 μg/ml), supporting the data obtained by FACE analysis (Fig. 4*C*).

ER stress. The majority of ER resident proteins are retained in the ER through a retention motif composed of four amino acids at the end of the chaperone protein sequences. The most common retention sequence is KDEL (Lys-Asp-Glu-Leu). During the ER stress response, these resident proteins are synthesized and secreted into the cytoplasm (53). To show whether continuous HA production from IPAH PASMCs is related to ER stress, we studied the expression of KDEL sequence containing glucose-regulated proteins GRP 78 and GRP 96 in PASMCs from patients with IPAH and controls. Figure 10 is a Western blot of protein expression from three IPAH and three control PASMC lysates. Expression of the KDEL sequence containing proteins GRP 78 and GRP 96 was not different between IPAH and control PASMCs. This suggests that high HA production in IPAH PASMCs is not related to ER stress, which is known to stimulate the HA cable response (32).

DISCUSSION

The pathogenesis of IPAH is not fully understood. The disease is typified by SMC proliferation and vascular remodeling. Although PASMCs are considered a major component of the remodeling process in IPAH, the processes by which PASMCs affect vascular proliferation and remodeling are not entirely clear. Our data suggest that HA metabolism by PASMCs in IPAH is abnormal resulting in high levels of HA in plasma and likely in the ECM. Enhanced interaction of

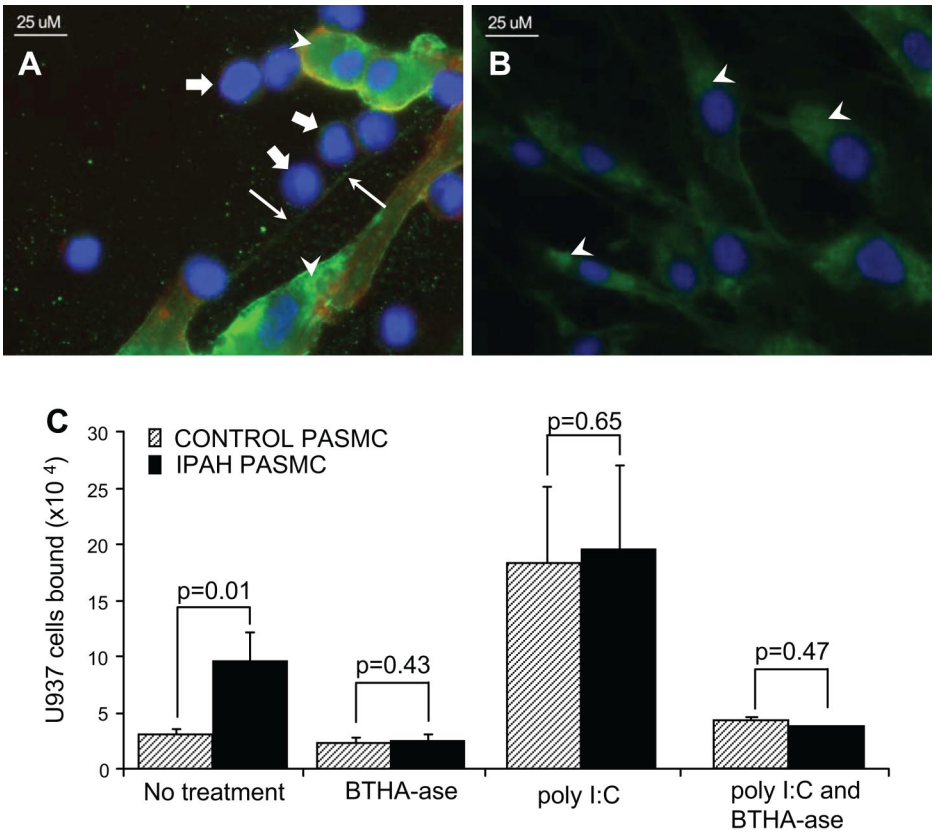

Fig. 5. U937 monocytic cells bind to HA produced by IPAH PASMCs. Fluorescence light microscopic images demonstrate binding of U937 monocytic cells (blue nuclei, thick arrows) to HA cables produced by IPAH PASMCs (*A*). Healthy control PASMCs make few if any HA cables for the U937 cells to bind (*B*). Adhesion of radiolabeled U937 cells was much higher in IPAH than controls. This binding was HA-specific as it was abrogated by the addition of the HA-specific enzyme, bovine testicular hyaluronidase (BTHA-ase). Polyinosinic acid:polycytidylic acid [poly(I:C)] stimulation of IPAH and control cells resulted in enhanced mononuclear cell binding. This binding was also HA-specific as it was abrogated by BTHA-ase treatment (*C*).

inflammatory cells with an increased HA matrix may contribute to the pathobiology of IPAH.

The key findings in our study are that patients with IPAH have significantly higher levels of circulating HA compared with controls. Furthermore, unstimulated PASMCs from IPAH patients produce HA cables that are capable of promoting mononuclear cell binding.

The levels of HA in the plasma of our controls were similar to normal plasma HA concentrations in adults reported in the literature (22, 30). In contrast, we found markedly increased HA concentrations (~10-fold) in plasma HA from patients with IPAH. These levels are similar to those reported in inflammatory conditions, including inflammatory bowel disease, asthma, and atherosclerosis (1, 9, 16, 29, 42, 47).

There are several possible explanations for the high levels of circulating HA in IPAH. In the lung, analysis of bronchoalveolar lavage (BAL) fluid from patients with sarcoidosis, idiopathic pulmonary fibrosis, and asthma revealed high HA levels related to the intensity of the alveolitis and with clinical severity (42). It was postulated that the presence of HA in BAL fluid in interstitial lung diseases may reflect fibroblast activation and/or proliferation (4). Since fibroblast activation is not a known major feature of IPAH, this is an unlikely mechanism in our patients. High HA levels have also been reported in liver

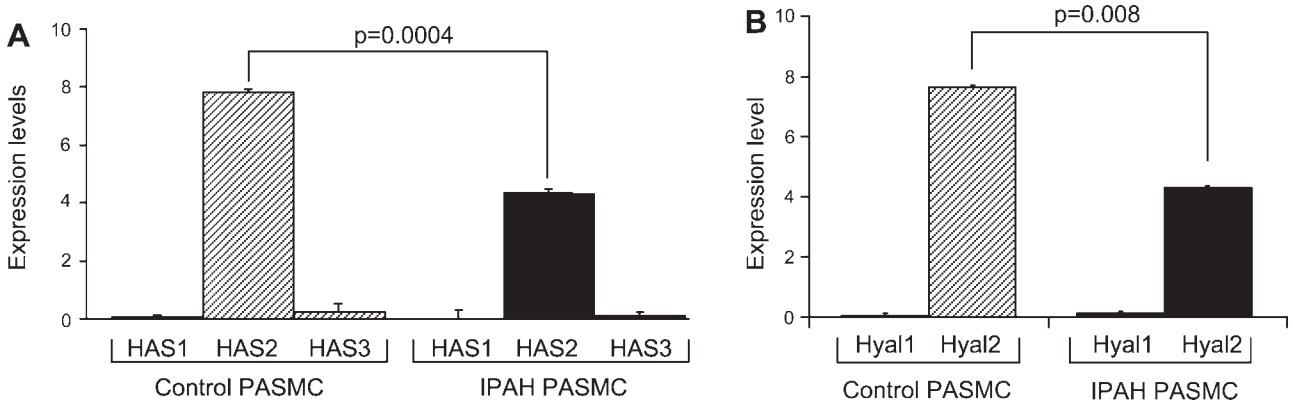

Fig. 6. HA synthase (HAS) and hyaluronidase (HYAL) expression in IPAH and control PASMCs. Real-time quantitative PCR SYBR Green analysis was done to determine the expression of HAS1, HAS2, HAS3, HYAL1, and HYAL2 genes in both control and IPAH PASMCs. Expression values and experimental error were calculated using GAPDH as a control for the amount of cDNA. HAS2 is the predominant HAS in both IPAH and control PASMCs, and expression levels are lower in IPAH (*A*). HYAL2 is the predominant HYAL in both IPAH and control PASMCs, and expression levels are lower in IPAH (*B*).

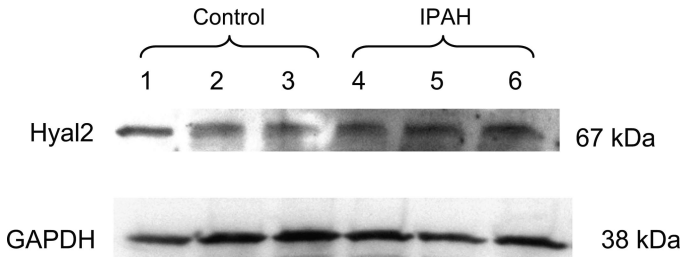

Fig. 7. Western blot analysis for HYAL2 from IPAH and control lungs. Proteins were separated by SDS-PAGE and transferred to a nitrocellulose membrane. The membranes were probed with rabbit anti-HYAL2 antibody. *Lanes 1–3* are from control PASMCs, and *lanes 4–6* are from IPAH PASMCs. Expression of HYAL2 was not different between IPAH and control PASMCs. Equal loading is demonstrated by GAPDH.

cirrhosis. Therefore, decreased clearance of HA by the liver or the kidney, the major routes of clearance of circulating HA (12, 29), may be another reason for elevated circulating HA levels. Although patients with severe IPAH may develop passive liver congestion and renal insufficiency, there was no evidence of liver cirrhosis or renal failure in any of our patients. All of our patients had normal liver function tests and creatinine levels. Our study population was limited to IPAH, and no cases of portopulmonary hypertension were included.

To better understand the source of these markedly elevated circulating HA levels in IPAH, we evaluated HA production by PASMCs and pulmonary artery endothelial cells (PAECs) from IPAH and control lungs. In our experiments, PAECs from IPAH and control lungs in culture did not produce significant levels of HA (data not shown). Interestingly, however, PASMCs from IPAH lungs spontaneously produced higher levels of HA and synthesized HA cables without stimulation. This was distinctly different compared with PAECs from IPAH and control lungs and with PASMCs from controls.

Since HA levels likely reflect a balance between production and degradation, we evaluated the expression levels of the various HAS enzymes that are responsible for HA synthesis and the HYALs that are responsible for its degradation. The fact that the predominant HAS (HAS2) and HYAL (HYAL2) were the same in PASMCs from both controls and IPAH likely reflects the known tissue specificities of these enzymes. Interestingly, in PASMCs from IPAH lungs, the expression of both HAS2 as well as HYAL2 were only approximately half of the levels seen in PASMCs from controls, whereas HYAL2 protein levels by Western analysis were similar in PASMC from IPAH and control lungs. Hyaluronidase activity in the plasma, however, was significantly lower in IPAH patients. This suggests that the high HA levels in IPAH are more likely due to decreased degradation than to increased production.

These findings confirm abnormalities in HA metabolism in PASMCs in IPAH, which brings up the question regarding the cause of these unusual abnormalities. Possibilities include inherent abnormalities in the PASMCs themselves in IPAH or abnormalities in the lung environment. Although both possibilities are plausible, our data could support both explanations.

In support of inherently abnormal PASMCs in IPAH, PASMCs from IPAH retain their ability to accumulate higher levels of HA when cultured ex vivo. If this phenomenon were purely a result of the lung environment such as high pulmonary artery pressures, it would be expected to be lost in culture,

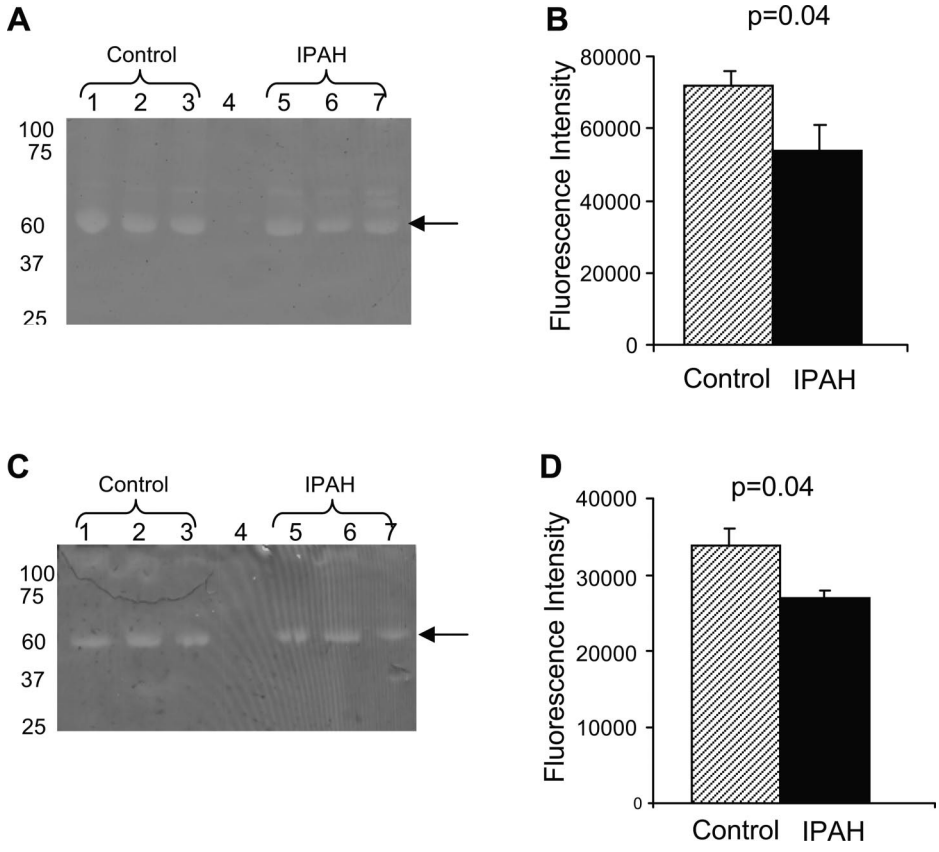

Fig. 8. Zymography for hyaluronidase. Hyaluronidase activity by zymography of plasma (*A*) and PASMC supernatants (*C*) from IPAH and controls. The white bands reflect HA clearance by hyaluronidase activity. Arrow shows the size of hyaluronidase (63 kDa) in control (*lanes 1–3*) and IPAH (*lanes 5–7*). No sample was loaded in *lane 4* as a negative control. The number on the *left* represents molecular mass markers in kilodaltons. Fluorescence intensities for plasma (*B*) and PASMC culture supernatant (*D*) were calculated by ImageJ program as described in EXPERIMENTAL PROCEDURES. The *P* value for the fluorescence intensities and standard errors were calculated from 4 experiments each done in triplicate. The hyaluronidase activity is significantly lower in plasma and PASMC supernatants from IPAH compared with controls.

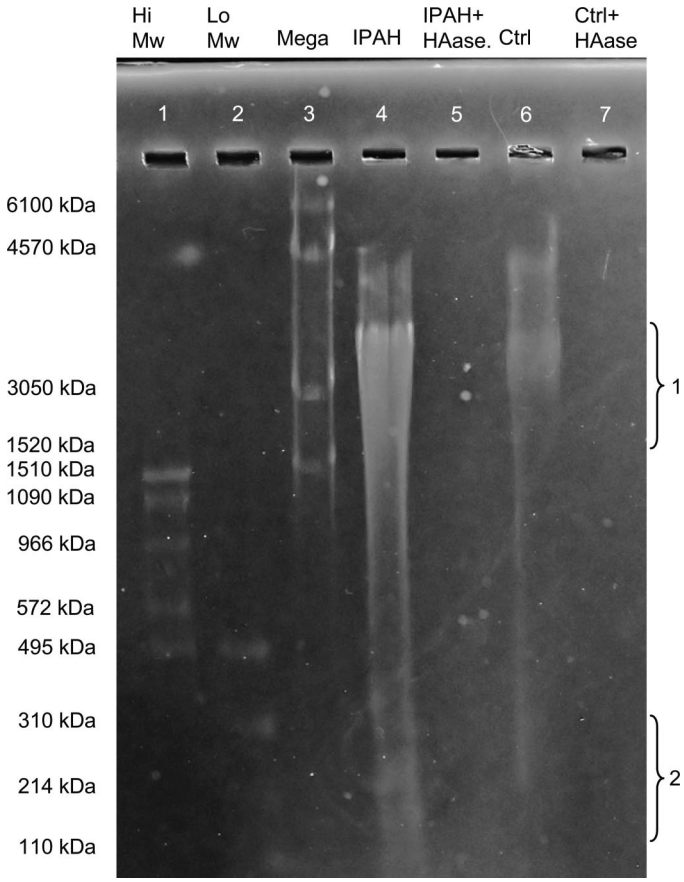

Fig. 9. HA sizing gel. IPAH (*lanes 4* and *5*) and control (*lanes 6* and *7*) PASMC lysates were loaded on 1% agarose gel. Samples in *lanes 5* and *7* had hyaluronidase added as negative controls. High (Hi Mw), low (Lo Mw), and Mega HA molecular mass markers were loaded in *lanes 1–3* as labeled. HA (HAase) in both IPAH and control (Ctrl) PASMCs is predominantly of very high molecular mass in the range of 3,050–4,570 kDa (bracket 1). In IPAH, there is also another less intense band in the range of 110–214 kDa (bracket 2).

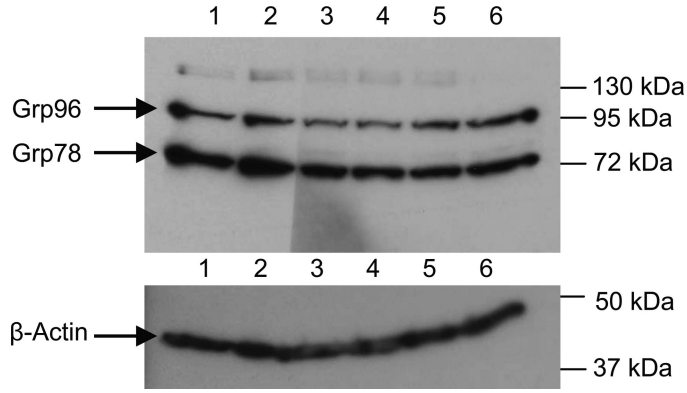

Fig. 10. Western blot analysis for KDEL (Lys-Asp-Glu-Leu) sequence containing glucose-regulated proteins GRP 78 and GRP 96 in PASMCs. PASMCs cell lysate from IPAH and control lungs were separated by SDS-PAGE gel and transferred to a nitrocellulose membrane. The membranes were probed with mouse anti-KDEL antibody. The locations of GRP 96 the GRP 78 as well as actin are indicated by arrows. *Lanes 1*, *3*, and *5* are from IPAH PASMCs, and *lanes 2*, *4*, and *6* are from control PASMCs. Expression of the KDEL sequence containing proteins GRP 78 and GRP 96 was not different between IPAH and control PASMCs. Equal loading is demonstrated by β-actin.

especially when the cells have been passaged. In support of abnormal lung environment, PASMCs from both control and IPAH lungs have a similar pattern of HAS and HYAL expression, and, when stimulated by poly(I:C), PASMCs from IPAH and control lungs produce similar levels of HA.

What is it in the lung environment that can have such an effect on PASMCs? In vitro studies show that stimulation of synthesis of HA by SMCs and endothelial cells can be in response to a variety of conditions (9) including inflammatory cytokines such as transforming growth factor-β_1 and PDGF (35, 44, 48), infectious agents (9), toxins (2, 27, 32, 41), hypoxia (15, 21, 36), or ER stress (32). Any of these factors may be responsible for the inherently high production of HA by PASMCs in IPAH. Local tissue hypoxia (real or perceived by the cells) is likely to have a major role. Whether it is systemic or local, hypoxia is a known feature of IPAH. It has also been reported that hypoxia induces HA synthesis (21). Furthermore, endogenous NO, which is known to be deficient in IPAH (18, 19, 26, 52), has an important role in hypoxia-enhanced HA synthesis (21). Hypoxia can stimulate the production of HA and the activity of hyaluronidase, which may promote angiogenesis (15), another major feature of IPAH.

Another recognized mechanism for increased production of HA by SMCs is ER stress (32). Our data, however, do not support this mechanism in IPAH PASMCs. This is based on our finding that expression of the KDEL sequence containing ER chaperone proteins GRP 78 and GRP 96 was similar in IPAH and control PASMCs. A more recently recognized mechanism for increased HA production in vitro is the presence of high glucose concentrations in the culture media (49). This is not the case in our cells since the glucose concentrations were lower than those known to be associated with increased HA production.

So what is the role of HA in the pathobiology of IPAH? Based on our data, there are several possibilities. HA consists of various molecular mass components in vivo especially in disease states. HA of different molecular masses may have

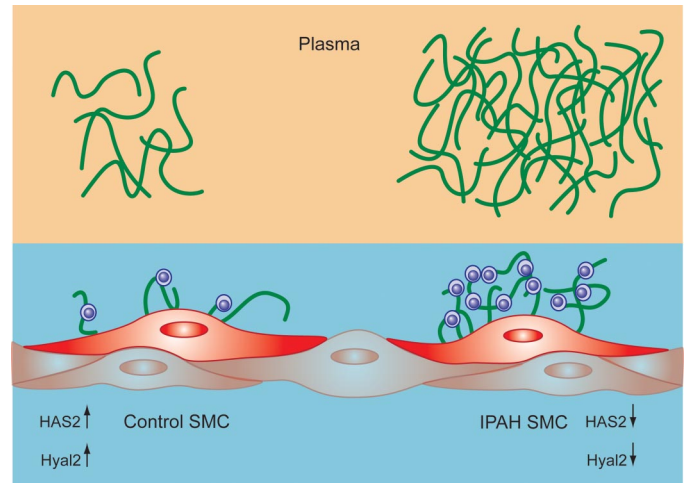

Fig. 11. Model of HA production and secretion by PASMCs from IPAH and control lungs. PASMCs from IPAH lungs spontaneously produce high levels of HA and have lower expression of HAS2 and HYAL2 compared with controls. IPAH patients have higher than normal levels of circulating HA in the blood, and PASMCs in culture secrete more HA into the media than control PASMCs.

very different physiological effects on cellular proliferation, migration, differentiation, as well as regulation of inflammation. Whereas large molecular mass HA is thought of more as a structural, wound healing, and remodeling molecule, HA with very low molecular mass has proinflammatory properties (43). Therefore, the size of HA that is upregulated in IPAH patient plasma and isolated PASMC can be helpful in understanding the potential role HA plays in IPAH.

Our finding that most of the HA in IPAH is in the very large molecular mass range (>1 million Da) suggests that HA plays a major structural role in remodeling and angiogenesis in IPAH. In support of this concept, tissue staining of the plexogenic lesions in IPAH revealed widespread staining for HA surrounding the lesions, but the area of most intense staining corresponded to areas of remodeling where there is medial destruction and new collagen deposition.

Interestingly, however, our work also shows that there is a small amount of low molecular mass HA in the PASMC lysates from IPAH. Furthermore, inflammatory cells can bind to HA produced by unstimulated PASMCs suggesting that HA produced by PASMCs in IPAH may serve a role in inflammatory cell binding to PASMCs. Since our untreated/unstimulated IPAH PASMCs constitutively express measurable amounts of HA on their surface that is also adhesive for inflammatory cells, we speculate that our cells are different, react differently to stimulation, or are induced by a different mechanism. Inflammation is a component in the pathobiology of IPAH. A significant inflammatory component is often reported in the periphery of plexiform lesions (11, 46). T cells, B cells, and macrophages seem to contribute to the inflammatory infiltrate in IPAH (11, 46). Inflammation is a common factor in the remodeling of all forms of severe and progressive IPAH (7, 46), and remodeling of the ECM in IPAH is considered to be caused by an ongoing local inflammatory process. Moreover, recent evidence indicates that CD44 on inflammatory cells can bind to HA-based cables and, in this way, engage leucocytes recruited to the tissue by an inflammatory stimulus (20).

In view of evidence that HA/CD44 can activate the RhoA/Rho kinase pathway (5), and that this signaling pathway is involved in mediating sustained pulmonary vasoconstriction in experimental models of pulmonary hypertension (23, 33, 34), it could also be speculated that the increased HA is inducing pulmonary vasospasm.

Thus HA produced by IPAH PASMCs could be involved not only in the structural changes of the remodeling process, but also as a component of the cellular recruitment, interactions, inflammation, and vasospasm.

Figure 11 depicts our proposed model of HA production and secretion by PASMCs from IPAH and control lungs. PASMCs from IPAH lungs spontaneously produce high levels of HA and have lower expression of HAS2 and HYAL2 compared with controls. IPAH patients have higher than normal levels of circulating HA in the blood, and PASMCs in culture secrete more HA into the media than control PASMCs. Thus, whereas all smooth muscles cells can produce HA on appropriate stimulation (9, 51), our novel data demonstrate that PASMCs from IPAH lungs produce high levels of HA without stimulation. This is an unusual and novel finding. Based on our findings in cultured cells, we believe that the source of high HA in IPAH patient plasma is likely the proliferating SMCs.

Our findings suggest that high levels of HA in patients with IPAH have an important role in the pathobiology of the disease and could serve as a biomarker of cellular proliferation and vascular remodeling. Furthermore, our findings reveal the important role of the matrix and the lung milieu in the pathobiology of IPAH and as potential targets for therapy aimed at halting or reversing cellular proliferation and vascular remodeling. Identification of the mediators that contribute to HA production and degradation could be useful in the development of new treatment or monitoring strategies in IPAH. These findings are particularly important in view of the fact that the future progress in IPAH therapy depends on our ability to target vascular remodeling in this disease.

ACKNOWLEDGMENTS

We thank J. Drazba for assistance with fluorescence imaging and confocal microscopy, H. Rho for help with FACE experiments, M. Lauer for assistance with the KDEL Western analysis and HA sizing, Kewal Asosingh for help with confirming SMC phenotype and purity, and M. Aronica for critical review of the manuscript.

GRANTS

This work was supported by National Heart, Lung, and Blood Institute Grants HL-68863 (R. A. Dweik), HL-60917 (S. C. Erzurum), and HL-081064 (S. C. Erzurum and V. C. Hascall).

REFERENCES

1. **Al'Qteishat A, Gaffney J, Krupinski J, Rubio F, West D, Kumar S, Kumar P, Mitsios N, Slevin M.** Changes in hyaluronan production and metabolism following ischaemic stroke in man. *Brain* 129: 2158–2176, 2006.
2. **Aridor M, Balch WE.** Integration of endoplasmic reticulum signaling in health and disease. *Nat Med* 5: 745–751, 1999.
3. **Armstrong SE, Bell DR.** Measurement of high-molecular-weight hyaluronan in solid tissue using agarose gel electrophoresis. *Anal Biochem* 308: 255–264, 2002.
4. **Bjermer L, Lundgren R, Hallgren R.** Hyaluronan and type III procollagen peptide concentrations in bronchoalveolar lavage fluid in idiopathic pulmonary fibrosis. *Thorax* 44: 126–131, 1989.
5. **Bourguignon LY.** Hyaluronan-mediated CD44 activation of RhoGTPase signaling and cytoskeleton function promotes tumor progression. *Semin Cancer Biol* 18: 251–259, 2008.
6. **Brecht M, Mayer U, Schlosser E, Prehm P.** Increased hyaluronate synthesis is required for fibroblast detachment and mitosis. *Biochem J* 239: 445–450, 1986.
7. **Caslin AW, Heath D, Madden B, Yacoub M, Gosney JR, Smith P.** The histopathology of 36 cases of plexogenic pulmonary arteriopathy. *Histopathology* 16: 9–19, 1990.
8. **de La Motte CA, Hascall VC, Calabro A, Yen-Lieberman B, Strong SA.** Mononuclear leukocytes preferentially bind via CD44 to hyaluronan on human intestinal mucosal smooth muscle cells after virus infection or treatment with poly(I. C). *J Biol Chem* 274: 30747–30755, 1999.
9. **de la Motte CA, Hascall VC, Drazba J, Bandyopadhyay SK, Strong SA.** Mononuclear leukocytes bind to specific hyaluronan structures on colon mucosal smooth muscle cells treated with polyinosinic acid:polycytidylic acid: inter-alpha-trypsin inhibitor is crucial to structure and function. *Am J Pathol* 163: 121–133, 2003.
10. **Deudon E, Berrou E, Breton M, Picard J.** Growth-related production of proteoglycans and hyaluronic acid in synchronous arterial smooth muscle cells. *Int J Biochem* 24: 465–470, 1992.
11. **Dorfmuller P, Perros F, Balabanian K, Humbert M.** Inflammation in pulmonary arterial hypertension. *Eur Respir J* 22: 358–363, 2003.
12. **Engstrom-Laurent A, Hellstrom S.** The role of liver and kidneys in the removal of circulating hyaluronan. An experimental study in the rat. *Connect Tissue Res* 24: 219–224, 1990.
13. **Evanko SP, Angello JC, Wight TN.** Formation of hyaluronan- and versican-rich pericellular matrix is required for proliferation and migration of vascular smooth muscle cells. *Arterioscler Thromb Vasc Biol* 19: 1004–1013, 1999.

14. **Farber HW, Loscalzo J.** Pulmonary arterial hypertension. *N Engl J Med* 351: 1655–1665, 2004.
15. **Gao F, Okunieff P, Han Z, Ding I, Wang L, Liu W, Zhang J, Yang S, Chen J, Underhill CB, Kim S, Zhang L.** Hypoxia-induced alterations in hyaluronan and hyaluronidase. *Adv Exp Med Biol* 566: 249–256, 2005.
16. **George J, Stern R.** Serum hyaluronan and hyaluronidase: very early markers of toxic liver injury. *Clin Chim Acta* 348: 189–197, 2004.
17. **Ghamra ZW, Dweik RA.** Primary pulmonary hypertension: an overview of epidemiology and pathogenesis. *Cleve Clin J Med* 70, *Suppl* 1: S2–S8, 2003.
18. **Giaid A, Saleh D.** Reduced expression of endothelial nitric oxide synthase in the lungs of patients with pulmonary hypertension. *N Engl J Med* 333: 214–221, 1995.
19. **Girgis RE, Champion HC, Diette GB, Johns RA, Permutt S, Sylvester JT.** Decreased exhaled nitric oxide in pulmonary arterial hypertension: response to bosentan therapy. *Am J Respir Crit Care Med* 172: 352–357, 2005.
20. **Hascall VC, Majors AK, De La Motte CA, Evanko SP, Wang A, Drazba JA, Strong SA, Wight TN.** Intracellular hyaluronan: a new frontier for inflammation? *Biochim Biophys Acta* 1673: 3–12, 2004.
21. **Hashimoto K, Fukuda K, Yamazaki K, Yamamoto N, Matsushita T, Hayakawa S, Munakata H, Hamanishi C.** Hypoxia-induced hyaluronan synthesis by articular chondrocytes: the role of nitric oxide. *Inflamm Res* 55: 72–77, 2006.
22. **Hasselbalch H, Hovgaard D, Nissen N, Junker P.** Serum hyaluronan is increased in malignant lymphoma. *Am J Hematol* 50: 231–233, 1995.
23. **Hemnes AR, Zaiman A, Champion HC.** PDE5A inhibition attenuates bleomycin-induced pulmonary fibrosis and pulmonary hypertension through inhibition of ROS generation and RhoA/Rho kinase activation. *Am J Physiol Lung Cell Mol Physiol* 294: L24–L33, 2008.
24. **Humbert M, Morrell NW, Archer SL, Stenmark KR, MacLean MR, Lang IM, Christman BW, Weir EK, Eickelberg O, Voelkel NF, Rabinovitch M.** Cellular and molecular pathobiology of pulmonary arterial hypertension. *J Am Coll Cardiol* 43: 13S–24S, 2004.
25. **Itano N, Sawai T, Yoshida M, Lenas P, Yamada Y, Imagawa M, Shinomura T, Hamaguchi M, Yoshida Y, Ohnuki Y, Miyauchi S, Spicer AP, McDonald JA, Kimata K.** Three isoforms of mammalian hyaluronan synthases have distinct enzymatic properties. *J Biol Chem* 274: 25085–25092, 1999.
26. **Kaneko FT, Arroliga AC, Dweik RA, Comhair SA, Laskowski D, Oppedisano R, Thomassen MJ, Erzurum SC.** Biochemical reaction products of nitric oxide as quantitative markers of primary pulmonary hypertension. *Am J Respir Crit Care Med* 158: 917–923, 1998.
27. **Kaufman RJ.** Orchestrating the unfolded protein response in health and disease. *J Clin Invest* 110: 1389–1398, 2002.
28. **Laurent TC, Fraser JR.** Hyaluronan. *FASEB J* 6: 2397–2404, 1992.
29. **Lindqvist U.** Is serum hyaluronan a helpful tool in the management of patients with liver diseases? *J Intern Med* 242: 67–71, 1997.
30. **Lindqvist U, Laurent TC.** Serum hyaluronan and aminoterminal propeptide of type III procollagen: variation with age. *Scand J Clin Lab Invest* 52: 613–621, 1992.
31. **Livak KJ, Schmittgen TD.** Analysis of relative gene expression data using real-time quantitative PCR and the 2(-Delta Delta C_T) method. *Methods* 25: 402–408, 2001.
32. **Majors AK, Austin RC, de la Motte CA, Pyeritz RE, Hascall VC, Kessler SP, Sen G, Strong SA.** Endoplasmic reticulum stress induces hyaluronan deposition and leukocyte adhesion. *J Biol Chem* 278: 47223–47231, 2003.
33. **McNamara PJ, Murthy P, Kantores C, Teixeira L, Engelberts D, van Vliet T, Kavanagh BP, Jankov RP.** Acute vasodilator effects of Rho-kinase inhibitors in neonatal rats with pulmonary hypertension unresponsive to nitric oxide. *Am J Physiol Lung Cell Mol Physiol* 294: L205–L213, 2008.
34. **Oka M, Homma N, Taraseviciene-Stewart L, Morris KG, Kraskauskas D, Burns N, Voelkel NF, McMurtry IF.** Rho kinase-mediated vasoconstriction is important in severe occlusive pulmonary arterial hypertension in rats. *Circ Res* 100: 923–929, 2007.
35. **Papakonstantinou E, Karakiulakis G, Roth M, Block LH.** Platelet-derived growth factor stimulates the secretion of hyaluronic acid by proliferating human vascular smooth muscle cells. *Proc Natl Acad Sci USA* 92: 9881–9885, 1995.
36. **Papakonstantinou E, Karakiulakis G, Tamm M, Perruchoud AP, Roth M.** Hypoxia modifies the effect of PDGF on glycosaminoglycan synthesis by primary human lung cells. *Am J Physiol Lung Cell Mol Physiol* 279: L825–L834, 2000.
37. **Patel S, Turner PR, Stubberfield C, Barry E, Rohlff CR, Stamps A, McKenzie E, Young K, Tyson K, Terrett J, Box G, Eccles S, Page MJ.** Hyaluronidase gene profiling and role of hyal-1 overexpression in an orthotopic model of prostate cancer. *Int J Cancer* 97: 416–424, 2002.
38. **Philipson LH, Schwartz NB.** Subcellular localization of hyaluronate synthetase in oligodendroglioma cells. *J Biol Chem* 259: 5017–5023, 1984.
39. **Quinn DA, Garg HG.** Hyaluronan in acute lung injury. In: *Yearbook of Intensive Care and Emergency Medicine*. Berlin: Springer Berlin/Heidelberg, 2006.
40. **Rich S, Dantzker DR, Ayres SM, Bergofsky EH, Brundage BH, Detre KM, Fishman AP, Goldring RM, Groves BM, Koerner SK, Levy PC, Reid LM, Vreim CE, Williams GW.** Primary pulmonary hypertension. A national prospective study. *Ann Intern Med* 107: 216–223, 1987.
41. **Ron D.** Translational control in the endoplasmic reticulum stress response. *J Clin Invest* 110: 1383–1388, 2002.
42. **Sahu S, Lynn WS.** Hyaluronic acid in the pulmonary secretions of patients with asthma. *Biochem J* 173: 565–568, 1978.
43. **Stern R, Asari AA, Sugahara KN.** Hyaluronan fragments: an information-rich system. *Eur J Cell Biol* 85: 699–715, 2006.
44. **Suzuki M, Asplund T, Yamashita H, Heldin CH, Heldin P.** Stimulation of hyaluronan biosynthesis by platelet-derived growth factor-BB and transforming growth factor-beta 1 involves activation of protein kinase C. *Biochem J* 307: 817–821, 1995.
45. **Teder P, Vandivier RW, Jiang D, Liang J, Cohn L, Pure E, Henson PM, Noble PW.** Resolution of lung inflammation by CD44. *Science* 296: 155–158, 2002.
46. **Tuder RM, Groves B, Badesch DB, Voelkel NF.** Exuberant endothelial cell growth and elements of inflammation are present in plexiform lesions of pulmonary hypertension. *Am J Pathol* 144: 275–285, 1994.
47. **Turino GM, Cantor JO.** Hyaluronan in respiratory injury and repair. *Am J Respir Crit Care Med* 167: 1169–1175, 2003.
48. **Usui T, Amano S, Oshika T, Suzuki K, Miyata K, Araie M, Heldin P, Yamashita H.** Expression regulation of hyaluronan synthase in corneal endothelial cells. *Invest Ophthalmol Vis Sci* 41: 3261–3267, 2000.
49. **Wang A, Hascall VC.** Hyaluronan structures synthesized by rat mesangial cells in response to hyperglycemia induce monocyte adhesion. *J Biol Chem* 279: 10279–10285, 2004.
50. **West DC, Hampson IN, Arnold F, Kumar S.** Angiogenesis induced by degradation products of hyaluronic acid. *Science* 228: 1324–1326, 1985.
51. **Wilkinson TS, Bressler SL, Evanko SP, Braun KR, Wight TN.** Overexpression of hyaluronan synthases alters vascular smooth muscle cell phenotype and promotes monocyte adhesion. *J Cell Physiol* 206: 378–385, 2006.
52. **Xu W, Kaneko FT, Zheng S, Comhair SA, Janocha AJ, Goggans T, Thunnissen FB, Farver C, Hazen SL, Jennings C, Dweik RA, Arroliga AC, Erzurum SC.** Increased arginase II and decreased NO synthesis in endothelial cells of patients with pulmonary arterial hypertension. *FASEB J* 18: 1746–1748, 2004.
53. **Yamamoto K, Fujii R, Toyofuku Y, Saito T, Koseki H, Hsu VW, Aoe T.** The KDEL receptor mediates a retrieval mechanism that contributes to quality control at the endoplasmic reticulum. *EMBO J* 20: 3082–3091, 2001.